European Journal of Pharmaceutical Sciences 78 (2015) 204–213

Contents lists available at ScienceDirect

European Journal of Pharmaceutical Sciences

journal homepage: www.elsevier.com/locate/ejps

Skin penetration behavior of lipid-core nanocapsules for simultaneous delivery of resveratrol and curcumin

Rossana B. Friedrich [a,b], Birthe Kann [a,c], Karine Coradini [a,b], Herman L. Offerhaus [c], Ruy C.R. Beck [b], Maike Windbergs [a,d,*]

[a] Saarland University, Department of Pharmacy, Biopharmaceutics and Pharmaceutical Technology, Campus A4.1, 66123 Saarbruecken, Germany
[b] Programa de Pós-Graduação em Ciências Farmacêuticas, Faculdade de Farmácia, Universidade Federal do Rio Grande do Sul (UFRGS), 90610-000 Porto Alegre, RS, Brazil
[c] University of Twente, Optical Sciences Group, MESA+ Institute for Nanotechnology, P.O. Box 217, 7500 AE Enschede, The Netherlands
[d] Helmholtz Centre for Infection Research and Helmholtz Institute for Pharmaceutical Research Saarland, Department of Drug Delivery, Campus A4.1, 66123 Saarbruecken, Germany

ARTICLE INFO

Article history:
Received 2 February 2015
Received in revised form 26 June 2015
Accepted 23 July 2015
Available online 26 July 2015

Keywords:
Resveratrol
Curcumin
Lipid-core nanocapsules
Co-encapsulation
Skin penetration
Cellular uptake

ABSTRACT

Polyphenols, which are secondary plant metabolites, gain increasing research interest due to their therapeutic potential. Among them, resveratrol and curcumin are two agents showing antioxidant, anti-inflammatory, antimicrobial as well as anticarcinogenic effects. In addition to their individual therapeutic effect, increased activity was reported upon co-delivery of the two compounds. However, due to the poor water solubility of resveratrol and curcumin, their clinical application is currently limited. In this context, lipid-core nanocapsules (LNC) composed of an oily core surrounded by a polymeric shell were introduced as drug carrier systems with the potential to overcome this obstacle. Furthermore, the encapsulation of polyphenols into LNC can increase their photostability. As the attributes of the polyphenols make them excellent candidates for skin treatment, the aim of this study was to investigate the effect of co-delivery of resveratrol and curcumin by LNC upon topical application on excised human skin. In contrast to the formulation with one polyphenol, resveratrol penetrated into deeper skin layers when the co-formulation was applied. Based on vibrational spectroscopy analysis, these effects are most likely due to interactions of curcumin and the stratum corneum, facilitating the skin absorption of the co-administered resveratrol. Furthermore, the interaction of LNC with primary human skin cells was analyzed encountering a cellular uptake within 24 h potentially leading to intracellular effects of the polyphenols. Thus, the simultaneous delivery of resveratrol and curcumin by LNC provides an intelligent way for immediate and sustained polyphenol delivery for skin disease treatment.

1. Introduction

Over the last years increasing research interest has been focused on polyphenols and their therapeutic potential. These secondary plant metabolites, present in fruits and vegetables as well as in red wine, act as effective free radical scavengers and play a beneficial role in preventing cardiovascular diseases, neurodegenerative disorders and cancer (Bisht et al., 2010). Amongst plant polyphenols, the phytoalexin resveratrol (trans-3,40,5-trihydroxys tilbene) has received considerable interest. This compound is naturally found in grapes, berries and peanuts and presents a wide range of pharmacological properties including antioxidant, anti-inflammatory, anti-aging and antimicrobial activity as well as potential chemopreventive effects against skin cancer (Amri et al., 2012). Curcumin (diferuloylmethane), another natural polyphenol, is a yellow pigment extracted from the rhizome of the turmeric plant *Curcuma longa* which is used as a popular spice in the South Asian cuisine (Amri et al., 2012). This promising non-toxic molecule has already successfully been used in Ayurvedic medicine for anti-inflammatory treatments. In addition, curcumin exhibits antioxidant, antibacterial, antimicrobial and

Abbreviations: LNC, lipid-core nanocapsules; B-LNC, blank lipid-core nanocapsules; RC-LNC, lipid-core nanocapsules loaded with resveratrol and curcumin; R-LNC, lipid-core nanocapsules loaded with resveratrol; C-LNC, lipid-core nanocapsules loaded with curcumin; RC-LNC$_R$ or RC-LNC$_C$, lipid-core nanocapsules loaded with resveratrol and curcumin but only data for one drug (resveratrol/curcumin) are discussed; RC-solution, resveratrol and curcumin in one solution; R-solution, resveratrol in solution; C-solution, curcumin in solution; RC-solution$_R$ or RC-solution$_C$, resveratrol and curcumin in solution but only data for one drug (resveratrol/curcumin) are discussed; CARS, coherent anti-Stokes Raman scattering; DMEM, Dulbecco's modified eagles medium; EE, encapsulation efficiency; FCS, fetal calf serum; NHDF-p, primary normal human dermal fibroblasts; SC, stratum corneum.

* Corresponding author at: Saarland University, Department of Biopharmaceutics and Pharmaceutical Technology, Campus A4.1, 66123 Saarbruecken, Germany.
E-mail address: m.windbergs@mx.uni-saarland.de (M. Windbergs).

http://dx.doi.org/10.1016/j.ejps.2015.07.018
0928-0987/

anticarcinogenic activity (Gupta et al., 2013). Besides the therapeutic potential of these individual substances, positive therapeutic effects of a combination of resveratrol and curcumin have previously been reported (Gupta et al., 2013; Iwuchukwu et al., 2011; Malhotra et al., 2010; Tavano et al., 2014). However, despite their beneficial properties, both polyphenols have limited clinical application due to their low water solubility and rapid metabolism within the human gastro-intestinal tract which result in poor systemic bioavailability and restrict their oral administration (Amri et al., 2012; Gupta et al., 2013).

To overcome these delivery obstacles, different nanoscale delivery systems including liposomes (Narayanan et al., 2009; Tavano et al., 2014), nanostructured lipid carriers (Wu et al., 2010), nanoemulsions, polymeric micelles and polymeric nanoparticles (Coradini et al., 2014; Detoni et al., 2012; Yallapu et al., 2012) have been described as strategies to improve the bioavailability, the pharmacological efficacy as well as the limited photostability of these polyphenols. Among these nanocarriers, special interest has been aroused on developing polymeric nanoparticles, either as solid spheres or capsules, based on biodegradable and biocompatible materials (Mora-Huertas et al., 2010).

In this context, a specific type of nanocapsules called lipid-core nanocapsules (LNC) has been introduced which are composed of an oily core surrounded by a polymeric shell stabilized by surfactants in aqueous medium (Jornada et al., 2012). LNC have shown high capacity to encapsulate poorly water soluble substances and have been proposed for systemic as well as for topical drug delivery (Detoni et al., 2012; Friedrich et al., 2014).

With respect to resveratrol, its encapsulation in LNC enabled higher deposition in the brain tissue of rats and showed promising effects in multiform glioblastoma and Alzheimer's disease models (Frozza et al., 2010, 2011). The nanoencapsulation of curcumin led to reduced tumor size and increased the animal survival rate in a pre-clinical model of gliomas (Zanotto-Filho et al., 2013). Considering the combination of polyphenols, Coradini et al. (2014) reported that nanoencapsulation enhanced the *in vitro* antioxidant activity of resveratrol and curcumin against $HO^{\cdot}$ radicals and a synergic effect was observed after co-encapsulation of both polyphenols. In addition, the co-encapsulation also improved the photostability of resveratrol (Coradini et al., 2014).

Against this background, the local delivery of resveratrol and curcumin in LNC via the human skin became interesting as a non-invasive alternative administration route, especially with respect to the local treatment of skin disorders including photocarcinogenesis, photoaging and sunburn (Nichols and Katiyar, 2010; Suwannateep et al., 2012).

Considering the topical application, initial *in vitro* studies showed the capacity of LNC to improve the photostability and promote the retention of resveratrol under UVA radiation (Detoni et al., 2012). However, to the extent of our knowledge, the interactions of such LNC and human skin, including the penetration and release of encapsulated actives, remains unexplored. As such investigations are mandatory for the development of effective dermal drug delivery via LNC, the objective of this study was to investigate the behavior of LNC co-encapsulating resveratrol and curcumin upon application onto excised human skin and their interactions with human primary skin cells. In addition, LNC loaded with the individual actives were investigated to evaluate the effect of co-administration.

2. Material and methods

2.1. Materials

Curcumin, sorbitan monostearate and poly(ε-caprolactone) (PCL) were obtained from Sigma–Aldrich (São Paulo, Brazil). Resveratrol was acquired from Pharma Nostra (Anápolis, Brazil) and polysorbate was supplied by Henrifarma (São Paulo, Brazil). Grape seed oil was acquired from Delaware (Porto Alegre, Brazil). Acetone, methanol and acetonitrile were purchased from Sigma–Aldrich (Steinheim, Germany). All chemicals and solvents were of pharmaceutical or HPLC grade and were used as received.

2.2. Preparation of lipid-core nanocapsules

Lipid-core nanocapsules were prepared according to the formulation reported by Coradini et al. (2014). In brief, 0.1 g polymer (PCL), 0.0385 g sorbitan monostearate as well as 165 μl of grape seed oil were dissolved in 27 ml of acetone at 40 °C. For the polyphenol-loaded formulations, resveratrol (0.005 g) curcumin (0.005 g) or the combination of both substances was added. This organic solution was poured into 54 ml of an aqueous phase containing 0.077 g polysorbate 80 under moderate stirring. Subsequently, acetone was evaporated and the aqueous phase was concentrated under reduced pressure to a final volume of 10 ml.

2.3. Characterization of lipid-core nanocapsules

The pH values were determined directly in the formulations using a calibrated potentiometer (VB-10, Denver Instrument, Arvada, USA). Particles size and polydispersity index of the samples were analyzed by photon correlation spectroscopy (PCS) (Zetasizer Nano ZS, Malvern Instruments, Malvern, UK) after dilution in ultrapure water (500 times dilution). The same instrument was used to measure the zeta potential by electrophoretic mobility after dilution of the formulations in 10 mM NaCl (500 times dilution). Further, nanoparticle tracking analysis (NTA) was performed (NanoSight LM 10 & NTA 2.2 Analytical Software, Malvern Instruments former Nanosight Ltd., Amesbury, UK) after diluting (5000×) the formulations in ultrapure water.

Morphological analysis was performed by transmission electron microscopy (TEM) (JEM JEM 2010, Tokyo, Japan) operating at 200 kV. For this analysis, the suspensions were diluted 200× in ultrapure water, placed on a specimen grid and negatively stained with phosphotungstic acid hydrate (1% w/v).

The drug content was assayed by ultra-high-performance liquid chromatography (UPLC) using Thermo Scientific Dionex UltiMate™ 3000 equipment. For resveratrol analysis, acetonitrile:acetic acid 2% (30:70, v/v) was used at a flow rate of 0.5 ml/min and the detection wavelength was 306 nm. The mobile phase used for curcumin was composed of methanol:acetic acid 2% (70:30, v/v) with a flow rate of 0.3 ml/min. The detection wavelength was 427 nm. The column used for both methods was a Purospher® STAR RP-18 endcapped (3 μm) Hibar® HR 50–2.1, kept at 30 °C. Total drug contents were determined after dissolution of nanoparticles (1 ml) in 10 ml acetonitrile. These solutions were maintained under stirring for approximately 20 min. After subsequent centrifugation, an aliquot of the supernatant was withdrawn, diluted in acetonitrile:water (50:50 v/v), filtered (0.22 μm) and 6 μl were injected in the UHPLC system.

The encapsulation efficiencies (EE, %) were determined by ultra filtration–centrifugation technique according to the previously reported protocol by Coradini et al. (2014). The percentage of polyphenol encapsulated was calculated by the difference between the total (content) and free polyphenol concentrations (ultrafiltrate) divided by the total polyphenol content and multiplied by 100 (Venturini et al., 2011).

The solubility of polyphenols in grape seed oil was determined by adding an excess of polyphenol powder (~30 mg) into 1 ml of oil. The dispersion was mixed for 2 min. After 24 h of storage in vertical position at room temperature, the samples were

centrifuged at 10,000 rpm for 10 min, and the supernatant was diluted 200 times in acetonitrile and analyzed by UPLC.

2.4. In vitro drug release study

The *in vitro* release studies of resveratrol and curcumin from different LNC were carried out with static Franz diffusion cells (15 mm diameter, type 4G-O1-00-20, Perme Gear, Riegelsville, PA, USA) with a diffusion area of 1.77 cm^2 and a receptor volume of 12 ml. Donor and receptor chamber were separated by a dialysis membrane (Mw cut off: 12–14,000 daltons, Medicell International Ltd, London, UK), previously saturated with water for 30 min. 500 µl of LNC suspension were placed in the donor compartment. The receptor medium was composed of PBS buffer pH 7.4 and ethanol (70:30 v/v) to guarantee sink conditions. At defined time points, samples (600 µl) were drawn from the receptor compartment and replaced with fresh medium. Air bubbles forming underneath the membrane were removed via the side arm. The experiments were performed over 24 h in triplicate at 32 °C and agitation of 400 rpm. Samples were diluted with acetonitrile (50:50 v/v) and analyzed using previously described UPLC conditions.

2.5. Cell culture

Primary normal human dermal fibroblasts (NHDF-p, Promocell C-12352, Heidelberg, Germany) were cultured in Dulbecco's modified Eagle medium (DMEM) supplemented with 10% fetal calf serum (FCS) in a 98% relative humidity atmosphere of 5% CO_2 at 37 °C. All materials were sterilized and LNC suspensions were prepared under aseptic conditions.

2.6. Colloidal stability of LNCs in biological medium

Before cell viability evaluation, the colloidal stability of lipid-core nanocapsules in cell culture medium was investigated. The suspensions were diluted 50 and 100 times in DMEM supplemented with 10% FCS. These concentrations were equivalent to 10 and 5 µg/ml of each polyphenol. Hydrodynamic diameter and polydispersity index (PDI) were measured by photon correlation spectroscopy immediately and 24 h after diluting the nanocapsules in cell culture medium.

2.7. Cell viability assay

Cell viability was examined by MTT ((3-(4,5-dimethylthiazol-2-yl)-2,5-diphenyltetrazolium bromide) assay. NHDF-p cells (passage 23) were seeded in 96-well plates (2×10^4 cells per well) and cultured for 72 h to reach semi-confluence. Cells were washed twice with PBS buffer and incubated with LNC suspensions for 24 h. LNC suspensions were directly diluted with cell culture media at concentrations of 5 and 10 µg/ml of each polyphenol. The control cells were treated with cell culture medium only (negative control), or with Triton X-100 (positive control). Subsequently, cells were washed with PBS buffer and incubated with MTT reagent (5 mg/ml in PBS pH 7.4) for 4 h. The precipitated formazan was dissolved with DMSO and quantified by measuring the absorbance at 550 nm in a plate reader (Tecan Deutschland GmbH, Crailsheim, Germany). The cell viability (%) was calculated in relation to the control culture without treatment (negative control), which represents 100% viability. Data are presented as mean of three samples ± standard deviation (SD) from three independent experiments.

2.8. Cellular uptake

30,000 NHDF-p cells (passage 9) were seeded in imaging dishes with a cover glass bottom and incubated with a 50 times diluted RC-LNC suspension. After 24 h, cells were washed and kept in medium during coherent anti-Stokes Raman scattering (CARS) microscopy analysis. The CARS microscope was equipped with a picosecond pulsed laser operating at a fundamental wavelength of 1032 nm (aeroPULSE-10, NKT Photonics, Birkerød, Denmark). Images were acquired with an Olympus 60× water immersion objective. The setup of the custom built CARS microscope has been described in detail elsewhere (Garbacik et al., 2012).

2.9. Skin penetration experiments

The penetration studies were performed in the static Franz diffusion cell system described above (Section 2.4) using full-thickness human skin and infinite-dose conditions. Abdominal skin samples were obtained from plastic surgery (Department of Plastic and Hand Surgery, Caritas-Krankenhaus, Lebach, Germany) with written consent of the patients and ethical approval of the Saarland medical association. Immediately after excision, the skin was prepared for storage at −26 °C until usage by removing the subcutaneous fat layer with a scalpel. Samples of one skin donor (female, 49 years old) were used for all experiments to reduce interindividual variability.

0.5 ml of R-LNC, C-LNC and RC-LNC were directly applied onto the skin in the donor compartment. In order to gain a better understanding of the co-encapsulation effect of resveratrol and curcumin on their skin penetration behavior, experiments were also carried out with 0.5 ml solutions (water:ethanol 50:50 (v/v)) of resveratrol (R-solution) and curcumin (C-solution) individually or in combination (RC-solution) containing 0.5 mg/ml of each polyphenol. As receptor medium, a mixture of PBS buffer pH 7.4 and ethanol (30%) was used. The abbreviations RC-solution$_R$ and RC-solution$_C$ were used to express the results for resveratrol or curcumin, respectively, from a solution containing the combination of both polyphenols.

After 24 h of incubation at 32 °C, the skin was carefully taken out of the cell and the excess formulation was removed with a swab. The stratum corneum (SC) was separated by tape stripping using 20 tapes and a weight of 2 kg placed centrally over the stripping delimited area (15 mm) for ten seconds. Then, a punch of 15 mm diameter was taken from the stripped area and viable epidermis and dermis were separated by heating the skin in a water bath at 60 °C for 90 s.

Resveratrol and curcumin were extracted from the skin by adding acetonitrile:acetic acid 2% (3:1, v/v), orbital shaking (120 min) and sonication (30 min) for tapes or by vortex mixing (90 s) and sonication (45 min) for viable epidermis and dermis, respectively. Moreover, the deeper skin layers (epidermis and dermis) were centrifuged for 15 min at 5000 rpm and the supernatant was collected for analysis. The polyphenols were quantified by UPLC described in Section 2.2 yielding an extraction recovery higher than 90% for all skin samples.

2.10. Infrared (IR) spectroscopy

Stratum corneum was separated following the protocol of Kligman and Christophel (1963) and subsequently incubated for 24 h in either pure ethanol or an ethanol water mixture (50:50(v/v)) with and without dissolved curcumin (1 mg/ml ethanol). IR spectra were recorded with 10 accumulations at three different sample positions using a FT-IR spectrometer (Spectrum 400, Perkin Elmer, Waltham, USA). All spectra were normalized to the peak at 1655 cm^{-1} in the IR spectrum of stratum corneum.

2.11. Statistical analysis

Statistical analysis was performed using analysis of variance (ANOVA) and Bonferroni test. A difference was considered statistically significant at the level of $p \leqslant 0.05$.

3. Results and discussion

For effective local application of polyphenols to human skin, LNC provide an elegant delivery approach as the photostability of the substances is increased and their *in vitro* antioxidant activity against HO· radicals which are harmful for skin cells is enhanced (Coradini et al., 2014). Further, as the lipophilic polyphenols can sufficiently be encapsulated into the delivery system due to the lipid core shell structure, no further organic solvents are required for the final application form.

3.1. Characterization of LNC suspensions

Lipid-core nanocapsules were prepared by interfacial polymer deposition using biodegradable and biocompatible materials approved by the U.S. Food and Drug Administration (FDA). Furthermore, previous *in vivo* studies indicate safety of the formulations for topical (Paese et al., 2009) as well as systemic application (Bulcão et al., 2013). The physicochemical characteristics of lipid-core nanocapsules are depicted in Table 1. All formulations presented a slightly acidic pH value, which is beneficial for topical application as it matches the skin surface pH (Schmid-Wendtner and Korting, 2006). The measured slight negative zeta potentials are in agreement with literature and potentially result from the coating of nanocapsules by polysorbate 80, giving them a steric stabilization at the particle/water interface (Friedrich et al., 2014; Venturini et al., 2011). Consequently, slight interactions between LNC and the skin can be expected, since the skin is slightly negatively charged (Honary and Zahir, 2013).

Lipid-core nanocapsules were also analyzed by NTA. The results (depicted in Fig. 1) confirm the data generated by PCS with mean particle sizes in the nanometer range as well as polydispersity indices ⩽0.12 indicating a narrow size distribution. The hydrodynamic diameters obtained by this technique were 183 ± 4 nm, 185 ± 14 nm, 185 ± 08 nm, and 181 ± 04 nm for B-LNC, R-LNC, C-LNC, and RC-LNC, respectively. The number of nanocapsules per milliliter was calculated for each formulation by multiplying the counted number of capsules considering the dilution (5000 times).

TEM images depict the spherical shape of the nanocapsules (Fig. 2). The mean particle size observed by TEM analysis was in agreement with those obtained by PCS and NTA. These results are in accordance with recently reported values for these formulations (Coradini et al., 2014).

3.2. In vitro drug release study

In vitro dissolution testing was performed using Franz diffusion cells with dialysis membranes separating donor and acceptor compartment. LNC suspensions were applied on top of the membrane in the donor compartment and samples from the acceptor compartment were withdrawn after predefined time intervals.

Comparing the release kinetics of the two different drugs revealed major differences (Fig. 3). 37.58% and 43.37% of resveratrol were released from R-LNC and RC-LNC after 6 h. However, less than 3% of curcumin were released from the respective LNC over the same time period. After 24 h, 58.47% and 73.43% of resveratrol were released from R-LNC and RC-LNC, respectively, whereas only 10.49% and 9.03% of curcumin were released from C-LNC and RC-LNC at the same time point.

The slower release of curcumin in comparison to resveratrol is consistent with results obtained by a dialysis bag method (Coradini et al., 2014). The differences in release kinetics can be correlated to the solubility of the individual polyphenols in grape seed oil constituting the lipophilic core of the nanocapsules. Solubility measurements with polyphenols and grape seed oil resulted in a solubility of 90 μg/ml for resveratrol and 475 μg/ml for curcumin, respectively. Consequently, the slower release of curcumin from the LNC can be related to the higher solubility in the oily carrier core compared to the aqueous dissolution medium.

The release profiles of curcumin from C-LNC and RC-LNC did not differ significantly. Thus, with regards to the co-encapsulation effect, the release profiles of curcumin were not influenced by the simultaneous presence of resveratrol ($p > 0.05$). In contrast, a significant difference in the release profiles of resveratrol was observed when both polyphenols were encapsulated in the same carrier. Whereas no differences between release profiles of R-LNC and RC-LNC was observable up to 6 h, the resveratrol release was significantly higher from RC-LNC beyond this time point ($p < 0.05$) suggesting a promoted release of resveratrol from RC-LNC triggered by co-encapsulation.

Therefore, the co-encapsulation of the polyphenols curcumin and resveratrol is an interesting strategy for skin application and was in the focus of a subsequent study investigating the interactions with human skin and the penetration behavior of the actives. The faster release of resveratrol may provide a controlled and immediate effect against free radicals, whereas curcumin could then provide a sustained source of an antioxidant agent over longer time intervals.

3.3. Colloidal stability investigations of LNC in biological medium

Maintaining physicochemical stability of nanoparticles in suspension is a prerequisite for the adequate evaluation of their potential biological effects (Allouni et al., 2009). Here, we analyzed if suspending LNC in cell culture medium supplemented with 10% FCS influenced size and PDI values of the lipid-core nanocapsules to avoid phenomena like agglomeration. PCS measurements were performed right after suspending LNC as well as after 24 h of storage in medium. LNC retained their size and narrow polydispersity indices (Table 2) for blank and loaded nanocapsules. Furthermore, results were similar to those obtained with LNC analyzed under

Table 1
Physicochemical properties and number of blank and drug-loaded lipid core nanocapsules (B-LNC, R-LNC, C-LNC, RC-LNC).

Formulation	B-LNC	R-LNC	C-LNC	RC-LNC	
Size (nm)	209 ± 0.07	202 ± 0.04	207 ± 0.06	201 ± 0.05	
PDI	0.12 ± 0.03	0.12 ± 0.01	0.12 ± 0.01	0.09 ± 0.02	
Zeta potential (mV)	−6.19 ± 0.17	−7.19 ± 1.19	−7.24 ± 0.74	−7.73 ± 0.73	
pH	6.34 ± 0.06	6.20 ± 0.03	6.28 ± 0.19	6.48 ± 0.09	
Drug loading (mg/ml)	–	0.48 ± 0.03	0.47 ± 0.03	Resveratrol	Curcumin
				0.49 ± 0.03	0.49 ± 0.01
Encapsulation efficiency (%)	–	99.79 ± 0.03	100 ± 0.00	99.80 ± 0.02	99.94 ± 0.08
Capsule number ($\times 10^{12}$)/ml	9.49 ± 0.68	9.53 ± 0.45	9.67 ± 0.21	9.70 ± 0.69	

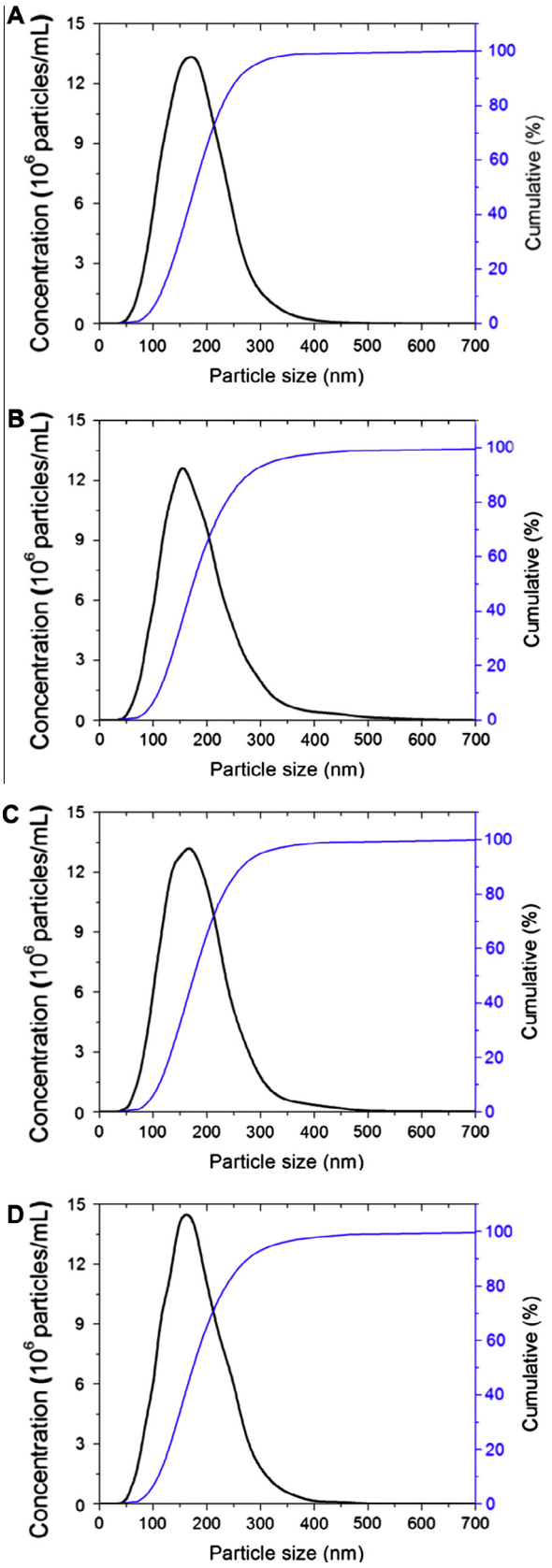

Fig. 1. Tracking analysis plots of (A) B-LNC, (B) R-LNC, (C) C-LNC, and (D) RC-LNC.

standard conditions (Table 1). Thus, the results indicate particle stability under standard cell culture conditions. This is likely due to steric hindrances based on polysorbate 80 micelles around the particles (Sabuncu et al., 2010). Polysorbate 80 is a non-ionic surfactant which attaches to the shell of lipid-core nanocapsules, thus providing steric stabilization (Venturini et al., 2011). In addition, polysorbate 80 coating of nanoparticles has been introduced as a strategy to modify body distribution of particles and to prevent protein plasma adsorption, thereby increasing their blood circulation time (Friedrich et al., 2014; Tröster et al., 1990).

3.4. Cell viability assay

As LNC are potentially taken up by cells after application via the skin, evaluating the toxicological potential of the nanocapsules is an important step towards the investigation of their efficacy at the cellular level. In our study, the cell viability of human dermal fibroblasts (NHDF-p cells) was investigated by an MTT assay, after NHDF-p cells were exposed to two different concentrations of each polyphenol (5 and 10 μg/ml) for 24 h. Subsequently, cell viability of the treated cells was calculated (Fig. 4). B-LNC did not show significant alterations in cell viability when compared to the untreated control group ($p > 0.05$). Moreover, the different polyphenol combinations or concentrations did not influence the cell viability in comparison to negative control cells ($p > 0.05$) either. Especially, as LNC with co-encapsulated polyphenols did not alter the cell viability profiles significantly, this delivery system bears a great potential for the simultaneous delivery of both actives.

3.5. Cellular uptake

In order to investigate potential cellular uptake of LNC, primary human skin cells (fibroblasts) were incubated with LNC suspension and coherent anti-Stokes Raman scattering (CARS) was applied as non-invasive chemically selective technique. CARS images were acquired at two frequencies to distinguish the lipid-core nanocapsules from the cell body. For this purpose, the protein band at 2928 cm^{-1} was excited to visualize the cell body (Fig. 5 left panels), whereas the frequency at 2845 cm^{-1}, which is characteristic for lipids, was chosen to image the LNC with a high contrast to their surroundings (Fig. 5 right panel). Fig. 5 shows the LNC uptake at different time points (A: 0 h; B and C: 24 h with different magnifications). By comparing left and right panels (especially in the close up images), the engulfed lipid-core nanocapsules are clearly distinguishable in the cell after 24 h. Due to the lipid core of the LNC, the excited anti-Stokes scattering becomes very intense in areas where LNC are located (Fig. 5, right panels). In contrast, these locations appear as the darkest parts in the left panels. The image contrast underlines the specificity of the chosen CARS frequencies to visualize the cellular LNC uptake. Overall, the LNC are taken up within 24 h in a reasonable quantity. They are localized in the cell cytosol and no evidence was found that LNC enter the nucleus. Furthermore, CARS images underline the results from the viability test, as morphological changes of the cells, which indicate decreasing cell viability, do not become visible. NHDF-p cells still show the elongated shape after 24 h exposure to LNCs which is typical for healthy fibroblasts.

3.6. Skin penetration

Considerable interest has been devoted to study the effects on skin upon topical application of free resveratrol and curcumin in different physiological and pathological conditions of skin (Narayanan et al., 2009; Ndiaye et al., 2011). Consequently, the main interest of this study was to evaluate the influence of the penetration behavior of the polyphenols within human skin when encapsulated in a delivery system. Thus, we investigated the skin penetration of nanocapsules containing resveratrol and curcumin

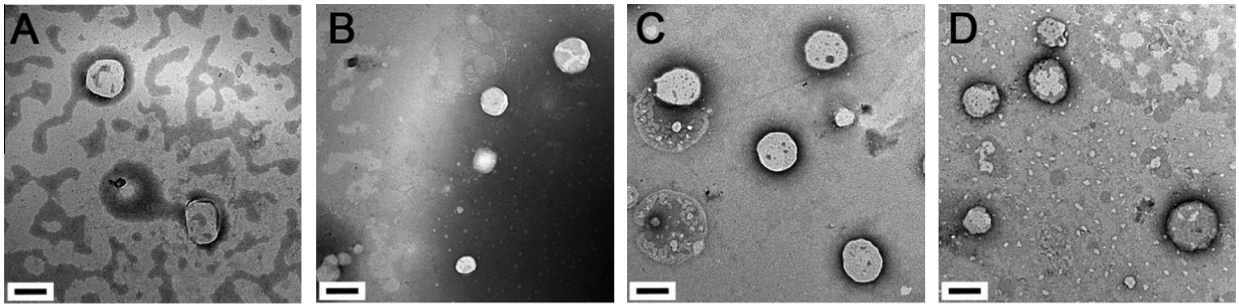

Fig. 2. Transmission electron micrographs of (A) B-LNC, (B) R-LNC, (C) C-LNC and (D) RC-LNC with 10,000× magnification (scale bar = 0.2 μm).

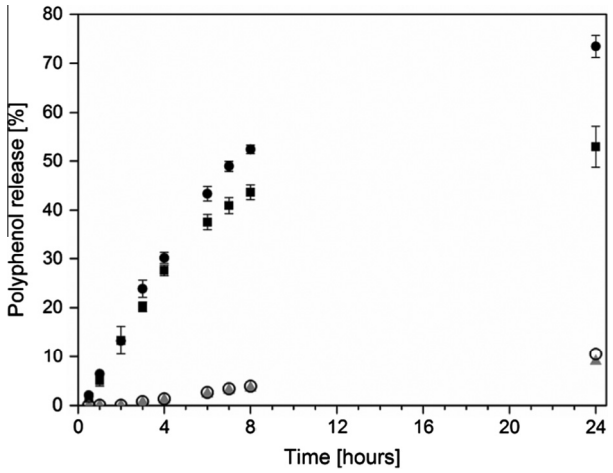

Fig. 3. *In vitro* release profiles of resveratrol and curcumin from lipid-core nanocapsules ($n = 3$) at 32 °C. Release from RC-LNC is depicted with circles (● resveratrol; ○ curcumin), whereas ■ and ▲ depict release curves for polyphenols from R-LNC and C-LNC, respectively. Standard deviations, which were always below 1.06%, are not shown for curcumin curves to maintain a clear data presentation.

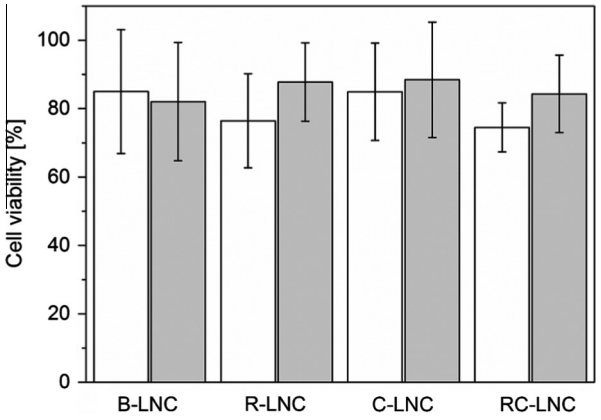

Fig. 4. NHDF-p cell viability after 24 h of incubation with blank and polyphenol-loaded LNC. B-LNC are diluted 50× (open bar) and 100× (gray bar), which is according to the tested two polyphenol concentrations 10 μg/ml (open bars) and 5 μg/ml (gray bars).

encapsulated as a single agent or in combination. For comparison, the skin penetration behavior of free polyphenols in solution was also tested.

Fig. 6 depicts the amount of polyphenols (μg/cm^2) which penetrated into the three skin layers: stratum corneum (SC) (Fig. 6A), viable epidermis (Fig. 6B) and dermis (Fig. 6C).

Overall, resveratrol and curcumin presented significantly different skin penetration behavior, regardless if the polyphenols were encapsulated or in their free forms ($p < 0.05$).

In stratum corneum, higher amounts of resveratrol applied as drug solution (R-solution: 1.19 ± 0.30 μg/cm^2; RC-solution$_R$: 1.07 ± 0.18 μg/cm^2) were found in comparison to encapsulated resveratrol (R-LNC: 0.52 ± 0.08 μg/cm^2; RC-LNC: 0.40 ± 0.06 μg/cm^2) as depicted in Fig. 6A left side. In the viable epidermis, the amount of resveratrol delivered by RC-LNC (0.69 ± 0.14 μg/cm^2) was significantly higher than resveratrol originating from single encapsulation and drug solution (R-solution: 0.33 ± 0.15 μg/cm^2, RC-solution$_R$: 0.43 ± 0.02 μg/cm^2 and R-LNC: 0.25 ± 0.07 μg/cm^2; $p < 0.05$) as depicted in Fig. 6B left side. Likewise, the same situation was found for resveratrol which penetrated into the dermis (Fig. 6C left side) (RC-LNC$_R$: 2.34 ± 0.74 μg/cm^2; R-solution: 0.76 ± 0.17 μg/cm^2, RC-solution$_R$: 1.26 ± 0.15 μg/cm^2 and R-LNC: 1.32 ± 0.20 μg/cm^2, $p < 0.05$).

The four bars on the right side in Fig. 6A–C depict the amount of curcumin per area (μg/cm^2) which penetrated into the different skin layers within 24 h after the application of drug solutions or lipid-core nanocapsules, respectively. In general, curcumin penetration into stratum corneum, viable epidermis and dermis was lower for LNC formulations compared to solutions ($p > 0.05$). 3.06 ± 0.62 μg/cm^2 and 2.61 ± 0.59 μg/cm^2 of curcumin applied in

Table 2
Size and polydispersity indexes (PDI) of lipid-core nanocapsules diluted in cell culture medium (100× and 50×).

	Polyphenol concentration (μg/ml)	0 h		24 h	
		Size (nm)	PDI	Size (nm)	PDI
B-LNC	–	207.2 ± 2.5	0.15 ± 0.01	212.0 ± 1.9	0.15 ± 0.01
	–	216.8 ± 1.7	0.16 ± 0.01	211.1 ± 0.8	0.12 ± 0.02
R-LNC	5	205.9 ± 0.6	0.14 ± 0.01	206.2 ± 2.3	0.15 ± 0.03
	10	210.5 ± 1.1	0.13 ± 0.01	217.4 ± 1.3	0.17 ± 0.01
C-LNC	5	216.8 ± 2.0	0.19 ± 0.00	205.5 ± 0.5	0.14 ± 0.01
	10	208.8 ± 1.1	0.12 ± 0.01	211.5 ± 0.8	0.11 ± 0.01
RC-LNC	5	232.7 ± 1.8	0.22 ± 0.00	225.4 ± 2.4	0.17 ± 0.03
	10	226.7 ± 1.5	0.17 ± 0.01	224.7 ± 0.7	0.16 ± 0.01

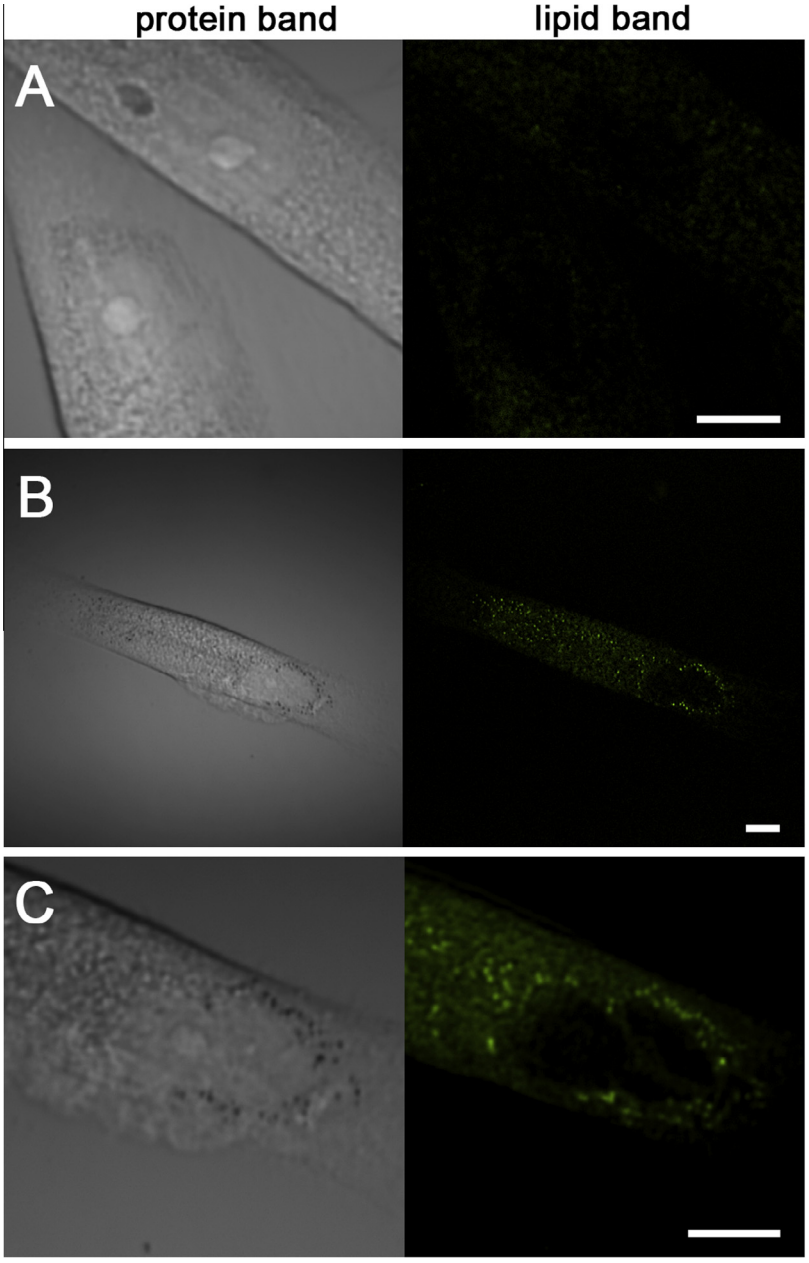

Fig. 5. CARS images of NHDF-p cells incubated with RC-LNC for 0 h (A) and 24 h (B: overview, C: close up). Left side depicts images acquired at the frequency of proteins (2928 cm^{-1}) showing the cell body. Right side shows images acquired at the lipid frequency (2845 cm^{-1}) depicting LNC with high contrast in false color. Scale bars are sized to 10 μm. (For interpretation of the references to color in this figure legend, the reader is referred to the web version of this article.)

solution on the skin (C-solution and RC-solution$_C$, respectively) were found in stratum corneum, whereas only 0.24 ± 0.06 μg/cm^2 and 0.29 ± 0.04 μg/cm^2 of curcumin originated from C-LNC and RC-LNC$_C$. Significantly higher amounts of curcumin deriving from polyphenol solutions were found in viable epidermis and dermis compared to curcumin which was released from LNC (C-solution: 1.59 ± 0.30 μg/cm^2/4.26 ± 0.88 μg/cm^2; RC-solution$_C$: 1.87 ± 0.29 μg/cm^2/3.68 ± 0.74 μg/cm^2; C-LNC: 0.16 ± 0.08 μg/cm^2/0.26 ± 0.05 - μg/cm^2; RC-LNC$_C$: 0.24 ± 0.18 μg/cm^2/0.46 ± 0.10 μg/cm^2).

It is striking that significantly higher amounts of curcumin applied in solution were found in all skin layers when compared to LNC. This phenomenon is due to differences in the diffusion processes for curcumin solution and loaded nanocapsules. Curcumin in solution was immediately available for skin penetration after application onto the skin. However, when curcumin was applied in its encapsulated form, the polyphenol had to be first released from the nanocapsule. Due to the slow diffusion out of the nanocapsule (Section 3.2), only low amounts of curcumin were able to penetrate into the skin within 24 h. Formulations containing both polyphenols (RC-solution and RC-LNC) did not influence the penetration behavior of curcumin in any of the three skin layers ($p > 0.05$) compared to the formulations containing only curcumin. The contrary was found for resveratrol. Here, the polyphenol combination in form of a solution did not affect the skin penetration behavior either ($p > 0.05$), whereas co-encapsulated resveratrol in form of nanocapsules was found in significantly higher amounts in viable epidermis and dermis than resveratrol applied as solution.

By comparing Fig. 6A–C for both polyphenols in solution, curcumin was found in larger quantities than resveratrol in all skin

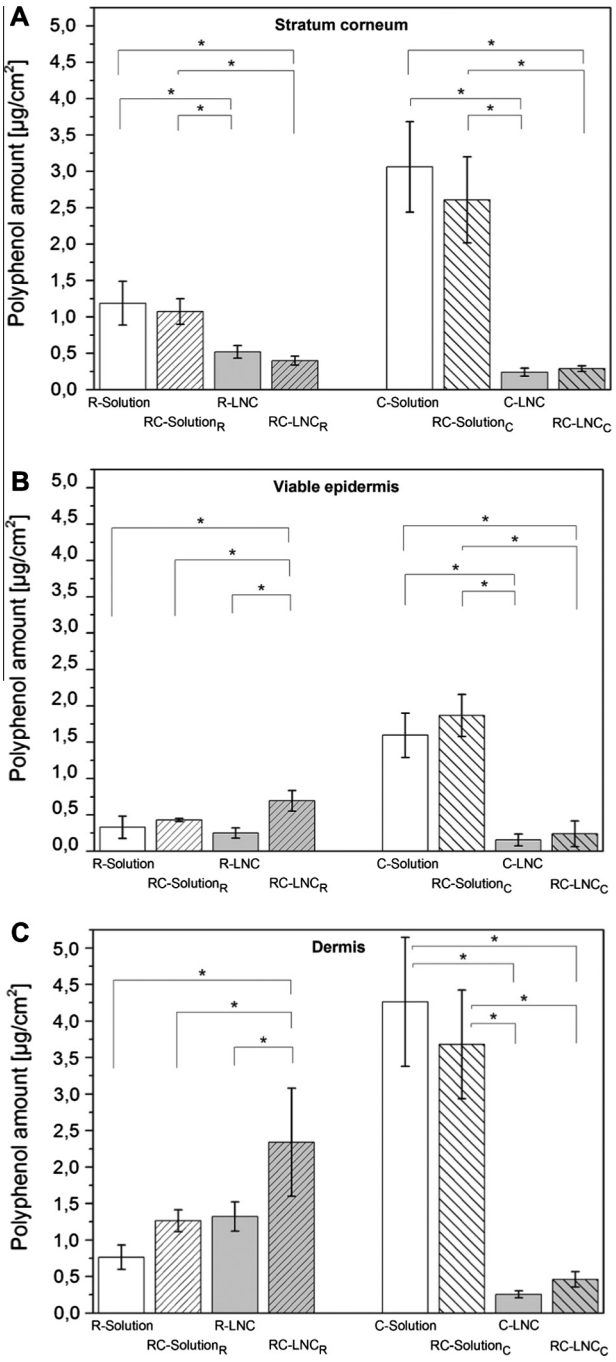

Fig. 6. Penetration of resveratrol and curcumin into different skin layers (A: Stratum corneum, B: Viable epidermis, C: Dermis) after 24 h of incubation with drug solutions or nanocapsules. Results are expressed as mean ± SD, $n = 3$. *Statistically different ($p < 0.05$).

layers. In stratum corneum, curcumin was found in 2.57 (C-solution) and 2.43 (RC-solution) times higher amounts than resveratrol (R-solution and RC-solution, respectively). Curcumin penetrated in 4.8 (C-solution) and 4.33 (RC-solution) times higher amounts into the viable epidermis than resveratrol applied in the respective solutions and in the dermis the amounts of curcumin were 5.57 and 2.91 times higher than resveratrol.

Overall, the penetration into all skin layers was higher for curcumin than for resveratrol, when polyphenols were applied in solution on the skin. An important factor was probably the different lipophilicities of the polyphenols. Taking this into account, the higher liposolubility of curcumin can provide a stronger affinity to the lipid bilayers of the stratum corneum, representing the most important barrier of the skin. After penetrating through the stratum corneum, possibly by following the intracellular route along the lipid bilayer, curcumin can penetrate further into deeper skin layers.

In contrast, the penetration behavior for both polyphenols encapsulated in lipid-core nanocapsules was opposed to the polyphenol solutions (Fig. 6). Here, resveratrol was found in larger quantities than curcumin in all skin layers. In stratum corneum, resveratrol was present in quantities 2.15 times (R-LNC) and 1.38 times (RC-LNC) higher than curcumin originating from the respective nanocapsule formulations (C-LNC and RC-LNC). In the viable dermis, resveratrol was found in 1.6 (R-LNC) and 2.91 (RC-LNC) times higher amounts than curcumin and in the dermis around 5 times higher.

In spite of polyphenol co-encapsulation (RC-LNC), the skin penetration behavior of curcumin was not modified ($p > 0.05$) compared to C-LNC. The opposite was observed for co-encapsulated resveratrol. Here, the penetration rate of the polyphenol into viable epidermis triplicated and doubled for the dermis ($p < 0.05$) in comparison to R-LNC.

The discrepancy in skin penetration behavior of the two polyphenols co-encapsulated can be related to different phenomena. The differences in the *in vitro* release profiles observed for each individual polyphenol lead to different amounts of drug freely available for skin penetration. Thus, the fast release kinetics of resveratrol provides a considerably higher amount for penetration at an early time point. Contrary, the lower amount of curcumin in all skin layers can be due to its slower *in vitro* release kinetics in relation to resveratrol.

As resveratrol delivered by R-LNC presented an increased penetration ability but not to the same extent as delivery by RC-LNC, the co-encapsulated curcumin states most likely a second causality. Curcumin potentially alters the structure of the phospholipid bilayer in the stratum corneum due to its good lipophilicity, thereby facilitating an easier and faster transport of resveratrol, which subsequently accumulates in the deeper skin layers. The high penetration capacity of resveratrol loaded-LNC is consistent with a previous study conducted over 8 h utilizing Franz diffusion cells and porcine skin (Detoni et al., 2012). In summary, our results support the assumption that the penetration of free molecules through the skin is mainly determined by their physicochemical properties and when the compounds are encapsulated, their skin absorption kinetics also depend on the release from the carrier system.

3.7. Infrared (IR) spectroscopy

Due to the observed discrepancy in skin penetration depth between resveratrol and curcumin, further analysis on the molecular basis was carried out. Infrared spectra were recorded to gain information about potential interactions or changes in the SC structure when exposed to polyphenols, as such effects are known for organic solvents (Megrab et al., 1995; Morimoto et al., 2002; Williams and Barry, 2012). As resveratrol is penetrating into deep skin layers in significantly higher amounts than curcumin (Section 3.6), it is likely that curcumin influenced SC components and thus facilitated the deeper penetration of resveratrol in the combined formulation.

The reference spectra of curcumin and stratum corneum are depicted in Fig. 7 (top spectra). The curcumin spectrum shows no significant overlap with characteristic peaks in the SC spectrum. Here, especially the amide I peak at around 1655 cm^{-1} (C=O stretch vibration) (Williams et al., 1992) as well as the peaks originating from symmetric and asymmetric CH-stretch vibrations at

about 2850 and 2920 cm^{-1}, respectively (Clancy et al., 1994; Mendelsohn et al., 2006), are important (highlighted with gray bars in Fig. 7A). The amide I band gives information about protein conformation, whereas bands arising from CH-stretch vibrations are associated with molecular conformation arrangements of skin lipids (Golden et al., 1986; Mendelsohn et al., 2006; Williams et al., 1992). As curcumin is water insoluble, curcumin dissolved in either 100% ethanol (EtOH) or a water:ethanol mixture (50%:50% (v/v)) was used to incubate excised human SC for 24 h, where the latter is the closest representation of our LNC formulation. To exclude structural changes within the SC samples caused by EtOH, SC was incubated in curcumin free solutions as well. Fig. 7A shows the full IR spectra, whereas panels B and C depict the enlarged peak regions of interest. A change of the amide I peak indicates conformational changes in proteins. Mendelssohn et al. observed a peak shift to lower wavenumbers in IR spectra due to conformational changes from α-helix to β-sheet structures, when SC was incubated with dimethylsulfoxide (Mendelsohn et al., 2006). In Fig. 7B a broadening and left shift of the amide I peak is visible compared to the references peak. The amide I peak in the spectrum of an intact protein in its native conformation is located at around 1655 cm^{-1}. A change or shift of this amide I peak indicates conformational changes in proteins. There is a difference in peak structure between SC incubated in water:ethanol with and without curcumin, indicating a potential curcumin influence in protein structural changes. It is unlikely that the shoulder and peak broadening arose due to the presence of curcumin, as curcumin peaks of similar intensity such as at about 1430 cm^{-1} did not become visible either. Due to the high ethanol content, these variations are hardly observable in the other IR spectra. However, a high ethanol content caused drastic peak intensity losses for the CH-stretch bands (Fig. 7C), which is probably linked to a lipid extraction from the SC due to the alcohol (Clancy et al., 1994). A reduced ethanol content did not reveal this intense spectral change.

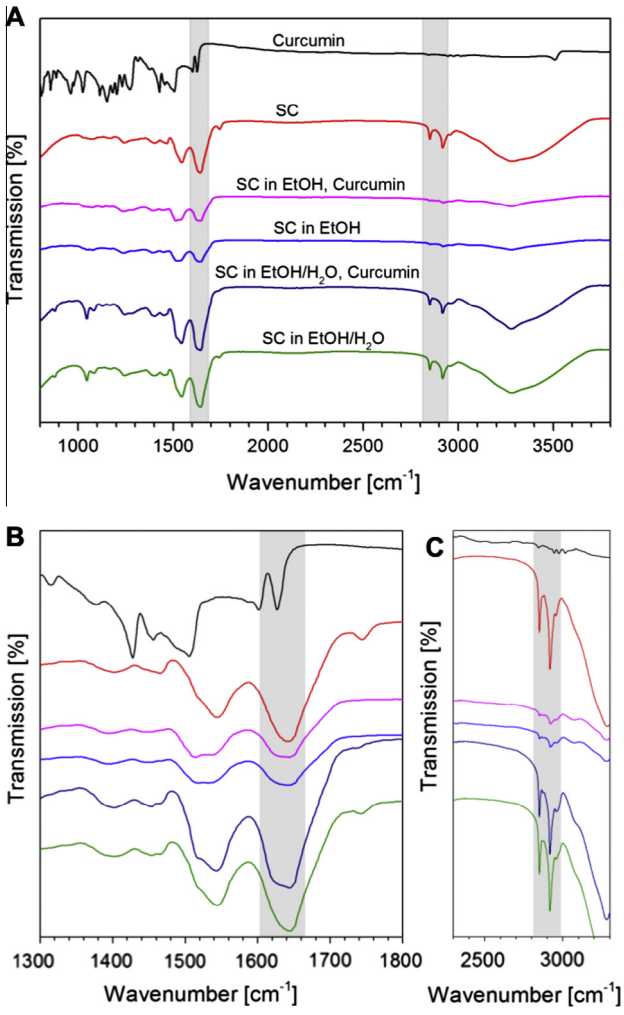

Fig. 7. IR spectra of curcumin, stratum corneum (SC) as well as SC incubated with curcumin containing and curcumin free solutions with different ethanol (EtOH) content. (A) Full IR spectra. (B) Enlarged section focusing on amide I peak. (C) Enlargement of CH-stretch vibration bands.

It has been reported that a change in the ratio of absorption intensities in CH-stretch vibrations indicates a relative lipid acyl chain disorder (Clancy et al., 1994; Yau, 1984). As IR spectra of SC show slightly more pronounced peak alterations in the presence of curcumin when compared to curcumin free solutions, it can be assumed that curcumin influences the lipid structure of SC. Thus, it is likely that curcumin mainly remains in upper skin layers where it alters SC properties and thus facilitates penetration of resveratrol across the stratum corneum into deeper skin layers upon co-delivery of the two polyphenols.

4. Conclusions

In conclusion, lipid-core nanocapsules were successfully fabricated with different polyphenol loading and characterized, providing high encapsulation efficiency as well as a narrow size distribution, which remained stable upon LNC dilution in biological medium. Upon interaction studies of LNC with human dermal fibroblast, lipid-core nanocapsules did not show cell toxic effects on fibroblasts. Skin cells engulfed LNC within 24 h, showing the great potential of this delivery system for further investigations on the subcellular level. *In vitro* drug release profiles showed a fast release for resveratrol, whereas curcumin was released slowly. The co-encapsulation led to an even faster release of resveratrol, while the curcumin release rate remained constant. Thus, due to the polyphenol combination an immediate as well as a sustained polyphenol release in one carrier system can be achieved. Skin penetration studies showed an increased delivery into deeper skin layers of resveratrol upon co-delivery in comparison to encapsulation of one individual polyphenol. Based on vibrational spectroscopy analysis, this phenomenon is most likely due to an interaction of curcumin with the lipid bilayers of the stratum corneum facilitating the penetration of the less lipophilic resveratrol across the major skin barrier into viable epidermis and dermis.

In light of these results, lipid-core nanocapsules bear a great potential as carrier systems for the delivery of low water soluble compounds like resveratrol and curcumin for local application to human skin.

Acknowledgements

The authors thank Dr. Chiara de Rossi for TEM image acquisition, Petra König for support with MTT tests and Peter Meiers for help with skin preparation. The German Academic Exchange Service (DAAD) and Coordenação de Aperfeiçoamento de Pessoal de Nível Superior (CAPES) are acknowledged for financial support.

References

Allouni, Z.E., Cimpan, M.R., Høl, P.J., Skodvin, T., Gjerdet, N.R., 2009. Agglomeration and sedimentation of TiO_2 nanoparticles in cell culture medium. Colloids Surf., B 68, 83–87.

Amri, A., Chaumeil, J.C., Sfar, S., Charrueau, C., 2012. Administration of resveratrol: what formulation solutions to bioavailability limitations? J. Controlled Release 158, 182–193.

Bisht, K., Wagner, K.H., Bulmer, A.C., 2010. Curcumin, resveratrol and flavonoids as anti-inflammatory, cyto- and DNA-protective dietary compounds. Toxicology 278, 88–100.

Bulcão, R.P., Freitas, F.A., Venturini, C.G., Dallegrave, E., Durgante, J., Göethel, G., Cerski, C.T.S., Zielinsky, P., Pohlmann, A.R., Guterres, S.S., Garcia, S.C., 2013. Acute and subchronic toxicity evaluation of poly(ε-Caprolactone) lipid-core nanocapsules in rats. Toxicol. Sci. 132, 162–176.

Clancy, M.J., Corish, J., Corrigan, O.I., 1994. A comparison of the effects of electrical current and penetration enhancers on the properties of human skin using spectroscopie (FTIR) and calorimetric (DSC) methods. Int. J. Pharm. 105, 47–56.

Coradini, K., Lima, F.O., Oliveira, C.M., Chaves, P.S., Athayde, M.L., Carvalho, L.M., Beck, R.C., 2014. Co-encapsulation of resveratrol and curcumin in lipid-core nanocapsules improves their in vitro antioxidant effects. Eur. J. Pharm. Biopharm. 88, 178–185.

Detoni, C.B., Souto, G.D., da Silva, A.L.M., Pohlmann, A.R., Guterres, S.S., 2012. Photostability and skin penetration of different E-resveratrol-loaded supramolecular structures. Photochem. Photobiol. 88, 913–921.

Friedrich, R.B., Dimer, F.A., Guterres, S.S., Beck, R.C.R., Pohlmann, A.R., 2014. Nanoencapsulation of tacrolimus in lipid-core nanocapsules showed similar immunosuppressive activity after oral and intraperitoneal administrations. J. Biomed. Nanotechnol. 10, 1599–1609.

Frozza, R.L., Bernardi, A., Paese, K., Hoppe, J.B., da Silva, T., Battastini, A.M., Pohlmann, A.R., Guterres, S.S., Salbego, C., 2010. Characterization of trans-resveratrol-loaded lipid-core nanocapsules and tissue distribution studies in rats. J. Biomed. Nanotechnol. 6, 694–703.

Frozza, R.L., Salbego, C., Bernardi, A., Hoppe, J.B., Meneghetti, A., Battastini, A.M., Guterres, S., Pohlmann, A., 2011. Incorporation of resveratrol into lipid-core nanocapsules improves its cerebral bioavailability and reduces the Aβ-induced toxicity. Alzheimer's Dement. 7, S114.

Garbacik, E.T., Herek, J.L., Otto, C., Offerhaus, H.L., 2012. Rapid identification of heterogeneous mixture components with hyperspectral coherent anti-Stokes Raman scattering imaging. J. Raman Spectrosc. 43, 651–655.

Golden, G.M., Guzek, D.B., Harris, R.R., McKie, J.E., Potts, R.O., 1986. Lipid thermotropic transitions in human stratum corneum. J. Invest. Dermatol. 86, 255–259.

Gupta, S.C., Patchva, S., Aggarwal, B.B., 2013. Therapeutic roles of curcumin: lessons learned from clinical trials. AAPS J. 15, 195–218.

Honary, S., Zahir, F., 2013. Effect of zeta potential on the properties of nano-drug delivery systems – a review (Part 1). Trop. J. Pharm. Res. 12, 9.

Iwuchukwu, O.F., Tallarida, R.J., Nagar, S., 2011. Resveratrol in combination with other dietary polyphenols concomitantly enhances antiproliferation and UGT1A1 induction in Caco-2 cells. Life Sci. 88, 1047–1054.

Jornada, D.S., Fiel, L.A., Bueno, K., Gerent, J.F., Petzhold, C.L., Beck, R.C.R., Guterres, S.S., Pohlmann, A.R., 2012. Lipid-core nanocapsules: mechanism of self-assembly, control of size and loading capacity. Soft Matter 8, 6646–6655.

Kligman, A.M., Christophel, E., 1963. Preparation of isolated sheets of human stratum corneum. Arch. Dermatol. 88, 702–705.

Malhotra, A., Nair, P., Dhawan, D.K., 2010. Modulatory effects of curcumin and resveratrol on lung carcinogenesis in mice. Phytother. Res. 24, 1271–1277.

Megrab, N.A., Williams, A.C., Barry, B.W., 1995. Oestradiol permeation across human skin, silastic and snake skin membranes: the effects of ethanol/water co-solvent systems. Int. J. Pharm. 116, 101–112.

Mendelsohn, R., Flach, C.R., Moore, D.J., 2006. Determination of molecular conformation and permeation in skin via IR spectroscopy, microscopy, and imaging. Biochim. Biophys. Acta 1758, 923–933.

Mora-Huertas, C.E., Fessi, H., Elaissari, A., 2010. Polymer-based nanocapsules for drug delivery. Int. J. Pharm. 385, 113–142.

Morimoto, Y., Wada, Y., Seki, T., Sugibayashi, K., 2002. In vitro skin permeation of morphine hydrochloride during the finite application of penetration-enhancing system containing water, ethanol and l-menthol. Biol. Pharm. Bull. 25, 134–136.

Narayanan, N.K., Nargi, D., Randolph, C., Narayanan, B.A., 2009. Liposome encapsulation of curcumin and resveratrol in combination reduces prostate cancer incidence in PTEN knockout mice. Int. J. Cancer 125, 1–8.

Ndiaye, M., Philippe, C., Mukhtar, H., Ahmad, N., 2011. The grape antioxidant resveratrol for skin disorders: promise, prospects, and challenges. Arch. Biochem. Biophys. 508, 164–170.

Nichols, J.A., Katiyar, S.K., 2010. Skin photoprotection by natural polyphenols: anti inflammatory, antioxidant and DNA repair mechanisms. Arch. Dermatol. Res. 302, 71–83.

Paese, K., Jäger, A., Poletto, F.S., Pinto, E.F., Rossi-Bergmann, B., Pohlmann, A.R., Guterres, S.S., 2009. Semisolid formulation containing a nanoencapsulated sunscreen: effectiveness, in vitro photostability and immune response. J. Biomed. Nanotechnol. 5, 240–246.

Sabuncu, A.C., Kalluri, B.S., Qian, S., Stacey, M.W., Beskok, A., 2010. Dispersion state and toxicity of mwCNTs in cell culture medium with different T80 concentrations. Colloids Surf., B 78, 36–43.

Schmid-Wendtner, M.H., Korting, H.C., 2006. The pH of the skin surface and its impact on the barrier function. Skin Pharmacol. Physiol. 19, 296–302.

Suwannateep, N., Wanichwecharungruang, S., Haag, S.F., Devahastin, S., Groth, N., Fluhr, J.W., Lademann, J., Meinke, M.C., 2012. Encapsulated curcumin results in prolonged curcumin activity in vitro and radical scavenging activity ex vivo on skin after UVB-irradiation. Eur. J. Pharm. Biopharm. 82, 485–490.

Tavano, L., Muzzalupo, R., Picci, N., de Cindio, B., 2014. Co-encapsulation of lipophilic antioxidants into niosomal carriers: percutaneous permeation studies for cosmeceutical applications. Colloids Surf., B 114, 144–149.

Tröster, S.D., Müller, U., Kreuter, J., 1990. Modification of the body distribution of poly(methyl methacrylate) nanoparticles in rats by coating with surfactants. Int. J. Pharm. 61, 85–100.

Venturini, C.G., Jäger, E., Oliveira, C.P., Bernardi, A., Battastini, A.M.O., Guterres, S.S., Pohlmann, A.R., 2011. Formulation of lipid core nanocapsules. Colloids Surf., A 375, 200–208.

Williams, A.C., Barry, B.W., 2012. Penetration enhancers. Adv. Drug Delivery Rev. 64 (Supplement), 128–137.

Williams, A.C., Edwards, H.G.M., Barry, B.W., 1992. Fourier transform Raman spectroscopy a novel application for examining human stratum corneum. Int. J. Pharm. 81, R11–R14.

Wu, X., Landfester, K., Musyanovych, A., Guy, R.H., 2010. Disposition of charged nanoparticles after their topical application to the skin. Skin Pharmacol. Physiol. 23, 117–123.

Yallapu, M.M., Jaggi, M., Chauhan, S.C., 2012. Curcumin nanoformulations: a future nanomedicine for cancer. Drug Discovery Today 17, 71–80.

Yau, D., 1984. Raman Spectroscopic Studies of Local Anaesthetic Model Biomembrane Interactions: A Study of the Roman Spectra of Model Biomembrane Systems Interacting with Local Anaesthetics Including Procaine and Tetracaine. Postgraduate School of Studies in Chemistry. University of Bradford, Bradford, p. 201.

Zanotto-Filho, A., Coradini, K., Braganhol, E., Schroder, R., de Oliveira, C.M., Simoes-Pires, A., Battastini, A.M., Pohlmann, A.R., Guterres, S.S., Forcelini, C.M., Beck, R.C., Moreira, J.C., 2013. Curcumin-loaded lipid-core nanocapsules as a strategy to improve pharmacological efficacy of curcumin in glioma treatment. Eur. J. Pharm. Biopharm. 83, 156–167.